Experimental Validation of Detecting Surface Deflections on Sheet Metal Parts with LS-Dyna

Annika Weinschenk[1], Agnes Schrepfer[1], Wolfram Volk[1]

[1]Chair of Metal Forming and Casting, Technical University of Munich, Walther-Meissner-Strasse 4, 85748 Garching, Germany

Abstract

The appearance of surface deflections on sheet metal parts is undesirable. When surface deflections are detected on a sheet metal part during tryout, the tool geometry has to be modified. This procedure is performed at a later stage of the product development process which leads to high costs and effort. Therefore, it is useful to detect surface deflections before the actual production in the finite element simulation. Then, it is much easier to modify the tool geometry in such a way that surface deflections don't occur any more.

In this paper, the reliability of the stoning method provided by LS-Dyna is investigated in a parameter study. The influence of the moving direction, the step size, the chosen area of the part for the stoning, the stone length, and the stone width on the detected surface deflections are analyzed. The results show that the chosen size of the area for the detection has a huge effect on the detected surface deflection. Similarly, the stone length has an influence but the stone width does not. To validate the finite element simulation, the strain distribution of the numerical part is compared to the physical part. The stoning method is applied to a physical part and the detected surface deflections are compared to those detected in the simulation. The study is conducted on a typically challenging part: a curved sheet metal part with a door handle depression.

1 Introduction

The visual appearance of a product is the first impression that a customer gets before he knows about it's specifications. A visible optical accuracy that is harmonious and aesthetical is highly important for a positive impression. This means that in sheet metal forming there are high expectations for outer panels regarding their surface quality as well as their function. Surface deflections are small geometrical deviations from the desired surface characteristic of a part. They become visible because they disturb the course of the reflected light from the area around them [1]. This is in contrast to the expectation of a harmonic course of the light on a part's surface.

Surface deflections occur during springback on huge, flat parts with small strains in the area of strong geometrical changes [2]. Compression stresses arise typically in the area around depressions where Springback occurs due to the small stiffness and small plastic strains [3]. The curvature of the part influences the position and visibility of these surface deflections [4]. Optical and tactile methods detect surface deflections on the physical part. While defects with a relatively huge depth, like wrinkles, can be identified easily, however, the detection of surface deflections is much more difficult because of their small depth.

2 Objective and Approach

The current state of research presents approaches to compensate surface deflections after first physical parts are produced and surface deflections are detected. To compensate these deflections, deep drawing tools are modified during tryout. Since this happens in a later stage of the product development process, it is time intensive. Therefore, it would be better to detect surface deflections in an early stage of the product development process using the finite element simulation [3]. It is then much easier to change the tool geometries before tool production. The accuracy of the detection of surface deflections in the simulation must be similar to the detection on physical parts. This paper investigates the influence of simulated stoning on the appearance of detected surface deflections. The results of the simulation are then compared to the experimental results.

The aim of an earlier study was to investigate the influence of the part geometry on the severity of occurring surface deflections [5]. The part geometry with clearly visible surface deflections is used for the study described in this paper. At first, an LS-Dyna simulation of the deep drawing process and the calculation of springback is conducted. After that, the stoning simulation is set up with the settings recommended in the LS-Dyna Keyword User's Manual [6]. Then, the settings are varied and the influence on the depth, dimension, and position of the surface deflections are analyzed. The physical part is produced and surface deflections are detected with the stoning method. The results of the experimental evaluation are compared to the numerical results.

3 Deep Drawing Process

Figure 1 shows the design of the deep drawing tool that is used to produce a part with multiple curves and a door handle depression. It consists of a lower part (a) and an upper part (b). The lower part includes the main components - punch and blank holder with a draw bead. The upper part consists of the outer and inner part of the die. A blank of AA6016 with a sheet thickness of 1.0 mm is used for the trials.

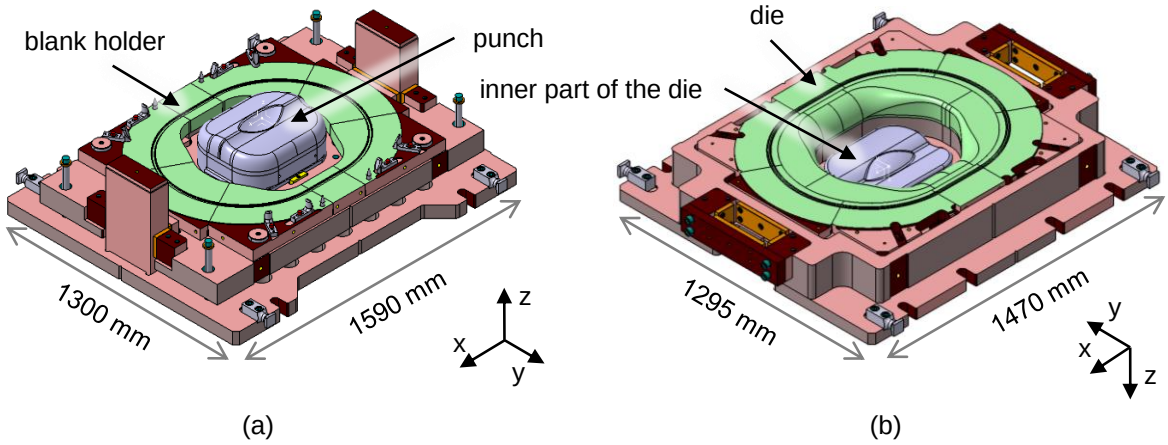

Fig.1: Lower part (a) and upper part (b) of the deep drawing tool

A blank holder force of 1,300 kN is chosen to lock the material flow through the draw bead. The traverse speed of the ram is 10 mm/s. Drawing oil and drawing foil are used to reduce friction. The drawing depth is 47.8 mm.

4 Finite Element Model

4.1 Deep Drawing Simulation

The deep drawing simulation is built in LS-Dyna. Figure 1 shows the complete deep drawing tool. The tool surfaces are cropped because not all surfaces get in contact with the blank. Figure 2 shows the essential surfaces for the numerical simulation. The blank has a size of 1000 mm x 800 mm. The model is symmetrical and therefore the y-z-plane through the origin of the coordinate system is used as a symmetry plane to reduce calculation time. The translation in x-direction and rotation about the local y- and z-axes is locked for all nodes in the symmetry plane.

The punch is fixed and the die and its inner part are moved in negative z-direction. The blank holder applies a force of 1,300 kN. ***CONTACT_ONE_WAY_SURFACE_TO_SURFACE** is used between the blank and each component of the tool. The Keyword ***MAT_3-PARAMETER_BARLAT_TITLE** is suitable to model the material AA6016 with a thickness of 1.0 mm. In the Keyword ***SECTION_SHELL,** the variable ELFORM is set to 16 for the blank and 2 for the rigid tools.

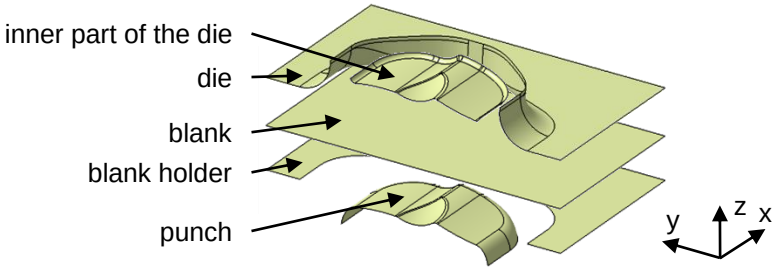

Fig.2: Surfaces of the deep drawing tool and blank for the finite element model

4.2 Springback Simulation

The constraints of the part after deep drawing are as follows. In addition to the symmetry described before, the translation of one node located in the symmetry plane is locked in x-, y-, and z-direction. At another node in the symmetry plane, the translation in x- and z-direction is locked.

4.3 Stoning Simulation

To detect surface deflections on the formed part after springback, the stoning method implemented in LS-Dyna is used. Therefore, the keyword **`*CONTROL_FORMING_STONING`** is necessary. Initially, the recommended settings from the LS-Dyna Keyword User's Manual [6] are used (Table 1).

Variable	Setting	Explanation
ISTONE	1	Calculation of the panel surface quality by using the stoning method. This is the only possible setting and therefore used.
LENGTH	150.0 mm	This is recommended in the manual.
WIDTH	30.0 mm	This is recommended in the manual.
STEP	0.5	The smallest element length is 0.5 mm. It is recommended to use an equal step size.
DIRECT	2	It is recommended to use two automatically defined stoning directions.
REVERSE	1	This reverses the part with consistent element normals.
METHOD	0	This is the curvature-based method and the only method available.
NODE 1 / NODE 2	0	This defines the direction of the movement of the stone. It is only necessary, if the automatically defined stoning direction is not used.
SETID		There is no recommendation for this variable, as the chosen set depends on the expected area of the surface deflections.
ITYPE	1	This depends on the chosen set, whether a node set (1) or element set (2) is chosen.

Table 1: Settings of the stoning simulation

It is recommended to use the SMOOTH option in the Keyword **`*CONTACT_FORMING_ONE_WAY_SURFACE_TO_SURFACE.`** Mesh adaptivity is not recommended in the SMOOTH/stoning areas. On the one hand, the element size must be sufficiently small to detect surface deflections. On the other hand, an entire mesh of small elements would lead to a significantly high number of elements because the blank size is huge. To determine a suitable mesh for the blank, a simulation of the deep drawing process with mesh adaptivity was conducted. The distribution of the element sizes on the final mesh after the deep drawing simulation was used as the initial mesh for the actual simulation. Thus, mesh adaptivity is not necessary any more. An average element size of 1 to 2 mm is recommended in the manual. However, in the actual simulation, a minimum element size of 0.5 mm was chosen. It is recommended that mass scaling with DT2MS needs to be sufficiently small to reduce the dynamic effect during forming. In this simulation no mass scaling was used to ensure that dynamic effects are as small as possible. The double precision version was used for this simulation as recommended.

5 Experimental Setup

5.1 Deep Drawing Process

A Dieffenbacher press was used for the experiments. Figure 3 (a) shows the press with the built-in deep drawing tool. Figure 3 (b) and (c) show respectively the upper part with the punch and blank holder, and the lower part with the die. Drawing oil was used in combination with a drawing foil of thickness 0.06 mm. The foil was cut to cover the relevant area between the blank and the punch as well as the blank and the inner part of the die.

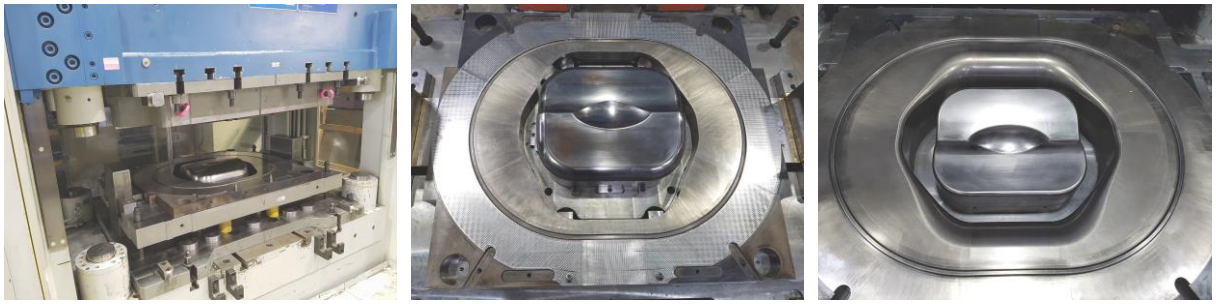

(a) (b) (c)

Fig.3: Deep drawing tool (a), upper part (b) and lower part (c) for the experiments

5.2 Strain Measurement

The strain distribution of the physical part and the numerical part are compared to validate the numerical results. A pattern was electrolytically etched onto the blank for measuring the strain with the GOM Argus system. It has a size of 390 mm x 270 mm to cover the relevant area of the depression and all other areas with possible surface deflections. The points of the pattern have a diameter of 1.0 mm and are spaced 2.0 mm apart.

6 Numerical and Experimental Evaluation

6.1 Numerical Evaluation

This section describes the results of the finite element analysis. At first, a stoning simulation with the recommended settings (as described in section 4.3) was conducted. The results are described in section 6.1.1. Afterwards, the settings for the stoning simulation were modified. The settings of the deep drawing simulation and the springback simulation remain unchanged. The influence of the stone length, stone width, direction of the stoning, step size, and a predefined set on the appearance of the detected surface deflections were investigated.

6.1.1 Results of the Stoning Simulation with the recommended Settings

Figure 4 (b) shows the right half of the sheet metal part with the detected surface deflections after the stoning simulation. The given fringe levels represent the depth of the surface deflections in mm. In area B the highest depth of the surface deflection is 0.1788 mm. Regarding the coordinate system with the origin in the centre of the full blank (Figure 4 (c)) the position of the node with the highest depth is x = 66.8 mm and y = 104.9 mm. The dimension of the surface deflection in x-direction is 128 mm and in y-direction it is 110.9 mm. In area A the maximum depth is 0.061 mm. The position of the node with the highest depth is x = 131.5 mm and y = -27.4 mm. The dimension in x-direction is 38.6 mm and in y-direction it is 28.1 mm.

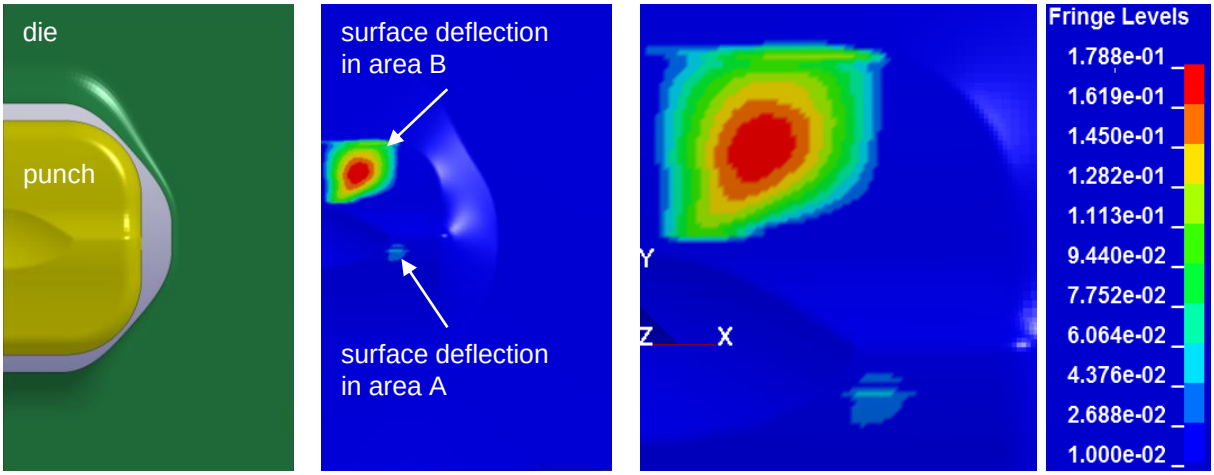

(a) (b) (c)

Fig.4: Appearance of the surface deflections on the sheet metal part after springback

6.1.2 Variation of the Stone Length

The recommended stone length is 150 mm [6]. For the investigation it was varied between 70 mm and 190 mm. Its influence on the maximum depth of the surface deflection in area B is shown in Figure 5. The chart shows that the stone with the smallest length of 70 mm detects a surface deflection of 0.109 mm. A higher stone length results in a higher depth until the maximum depth of 0.1788 mm is reached with a stone length of 140 mm. As described in 6.1.1, the x-dimension of the surface deflection is 128 mm. A stone with a length smaller than 128 mm will therefore not be able to detect the depth of the surface deflection correctly. The results also show that stones with a length smaller than 140 mm detect a smaller x-dimension while the y-dimension remains the same. To detect the maximum depth correctly, it is necessary that the stone length is higher than the x-dimension of the surface deflection. Since the x-direction of the surface deflection in area A is 38.6 mm, the detected maximum depth is the same for each tested stone length.

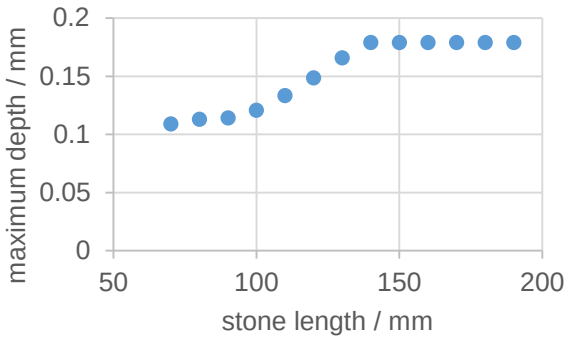

Fig.5: Influence of the stone length on the maximum depth of the surface deflection in area B

Figure 6 shows the influence of the stone length on the position of the node with the maximum depth of the surface deflection. It can be seen that a higher stone length detects a node further away from the origin of the coordinate system. The dependency is almost linear.

As Figure 4 shows, the width of the surface deflection is smaller in the lower area. This means, that even a stone with a smaller length can detect the surface deflection in this area correctly. Whereas in the upper area the width of the surface deflection is too wide to be detected by a stone with a small length. In the upper area, the stone fits completelly into the surface deflection. Therefore, it detects a smaller maximum depth. Because of this, a stone with a small length detects a higher maximum depth in the lower area of the surface deflection.

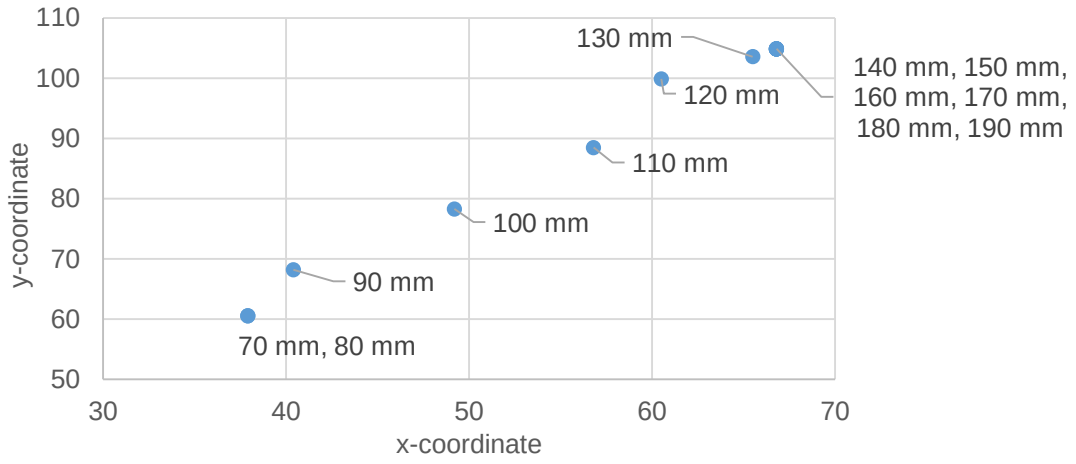

Fig.6: Influence of the stone length on the position of the node with the maximum depth of the detected surface deflection in area B

The results are different for the surface deflection in area A as there is no difference in the maximum depth, dimension and position for a variation of the stone length.

6.1.3 Variation of the Stone Width

The following stone widths were investigated: 1 mm, 5 mm, 10 mm, 15 mm, 20 mm, 25 mm, 30 mm, 35 mm, 40 mm, 45 mm, and 50 mm. A stone length of 150 mm is used for every simulation. All results show, that the stone width has no influence on the maximum depth, dimension and position of the surface deflections in area A and B. The reason could be, that the curvature in y-direction is so high, that the stone has always just a linear contact with the surface of the part. The stone width would have an influence, if either the surface would be almost flat or would be wavy.

6.1.4 Variation of the Stoning Direction

Four different directions of the stone movement were tested: One automatically determined direction (a), two automatically determined directions (b), a manually determined x-direction (c), and a manually determined y-direction (d). Figure 7 shows the results of the stoning simulation. It can be seen that three cases lead to the same result. The analysis using the automatically determined direction, the automatically determination of two directions and the manual determination of the stoning direction in x-direction detect the same surface deflections. A stoning in y-direction leads to a completely different result with no detected surface deflections. This proofs, that both the options “one automatically determined direction” and “two automatically determined directions” chose the x-direction for the movement of the stone. The x-direction is the direction of the minimum principal curvature. Therefore, the surface deflections are detected correctly then this direction is used.

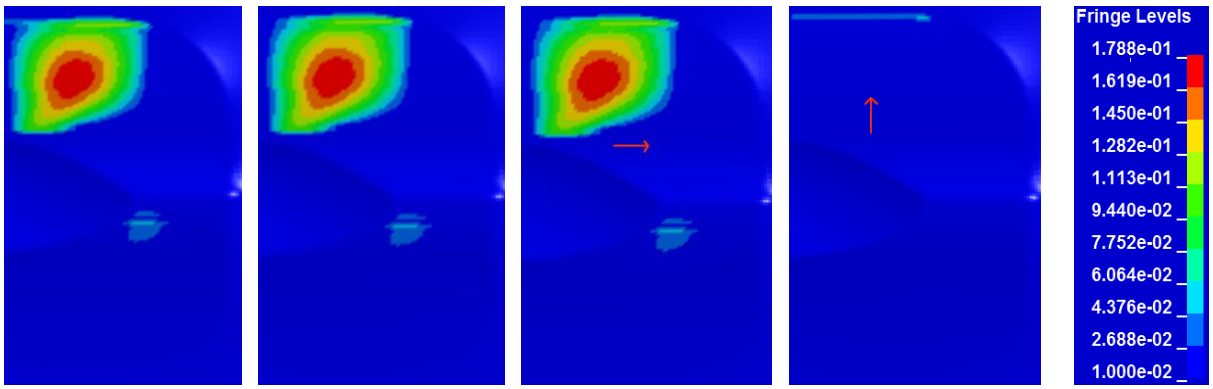

(a) (b) (c) (d)

Fig.7: Influence of the stoning direction on the appearance of surface deflections

6.1.5 Variation of the Step Size

Additionally, the step size of the stoning was modified. The following step sizes were used: 0.1 mm, 0.5 mm, 1.0 mm, 2.5 mm, 5.0 mm, 7.5 mm, and 10.0 mm. For 0.1 mm, 0.5 mm, and 1.0 mm the maximum depth in area B is nearly equal. However, for 2.5 mm, 5.0 mm, and 10.0 mm the maximum depth is also nearly the same but smaller than the one for the first three ones. For 10 mm the maximum depth is also smaller. The same applies to the depth of the surface deflection in area A. The step sizes 5.0 mm to 10.0 mm result in a smaller depth than the other step sizes. The distribution of the depth is homogeneous for the step sizes 0.1 mm to 5.0 mm. It can be seen that a higher step size leads to vertically stripes due to different detected depths.

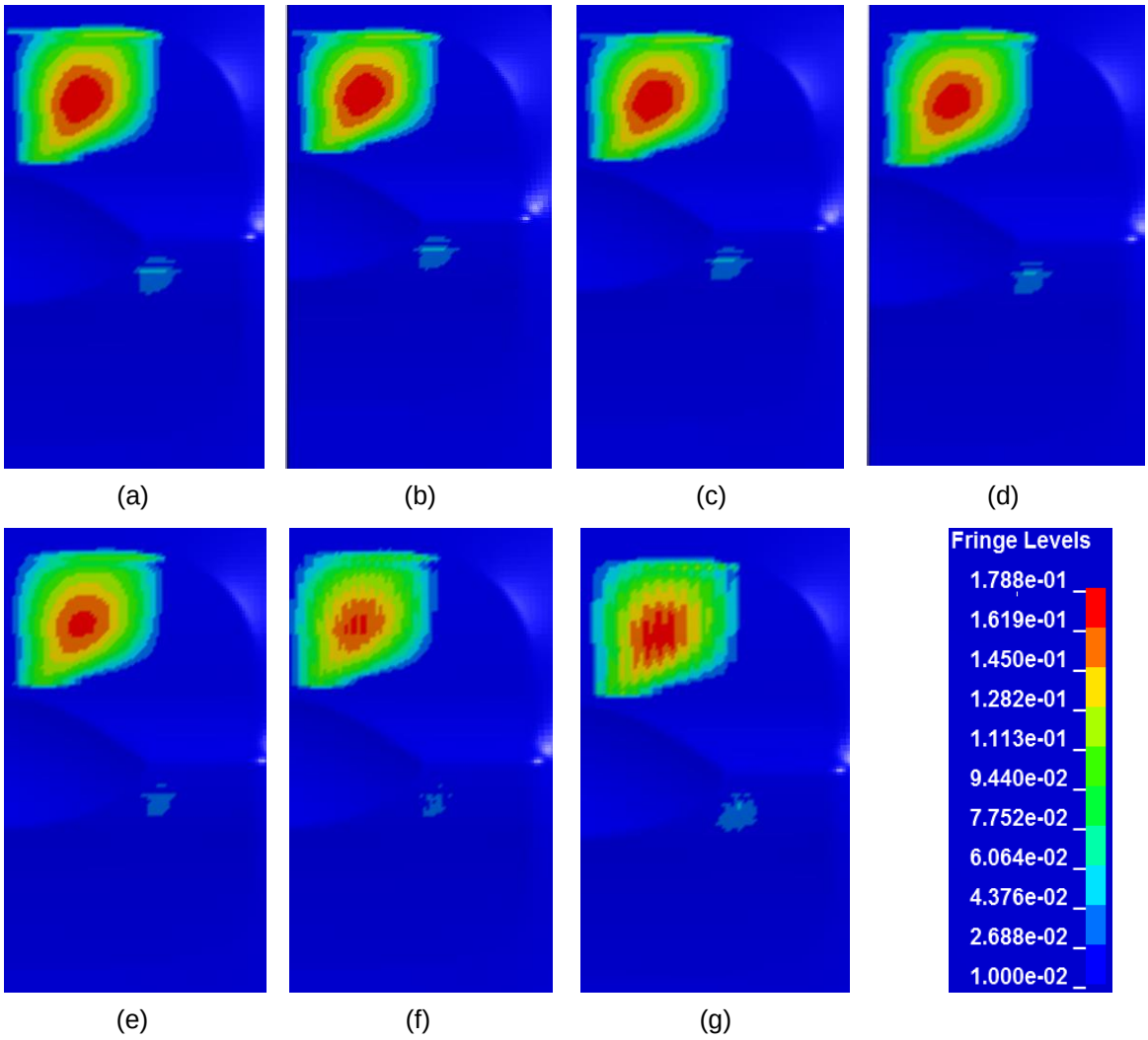

Fig.8: Influence of the variation of the step size on the appearance of surface deflections: 0.1 mm (a), 0.5 mm (b), 1.0 mm (c), 2.5 mm (d), 5.0 mm (e), 7.5 mm (f), 10.0 mm (g)

6.1.6 Variation of the Set

The area of the part, in which surface deflections should be detected, must always be given by the user, as there is no pre-set. Four sets with different sizes were investigated for both areas A and B. The first ones in Figure 9 (a) were already used for the simulations shown in Figures 4, 7, and 8. The two sets are in regions where surface deflections typically occur. They are large enough so that the surface deflections should be fully covered. Figure 9 (b) shows the results of the stoning simulation. The surface deflection in area A is smaller than the chosen size of the set. Whereas the surface deflection in area B is nearly as large as the set size. Figure 9 (c) shows a set in area A that is slightly smaller than the previously detected surface deflection. The set in area B is significantly smaller than the detected surface deflection. The results in Figure 9 (d) show that the surface deflection in area A is not detected any more. The surface deflection in area B is much smaller than the one in Figure 9 (b).

In Figure 9 (e) the sets cover the complete double positive curved areas in which surface deflections occur. The results shown in Figure 9 (f) illustrate that the surface deflection in area B is much larger and deeper than the one in Figure 9 (b). The surface deflection in area A is wider, but the depth is nearly the same. In Figure 9 (g) the whole surface of the part without the door handle depression was used as the investigated set. The results in Figure 9 (h) show that the surface deflections in area A and B are similar to the ones in Figure 9 (f). Two large red surface deflections are detected besides. The results of this study show that the selection of the set size has a huge effect on the detected depth and dimension of the surface deflections.

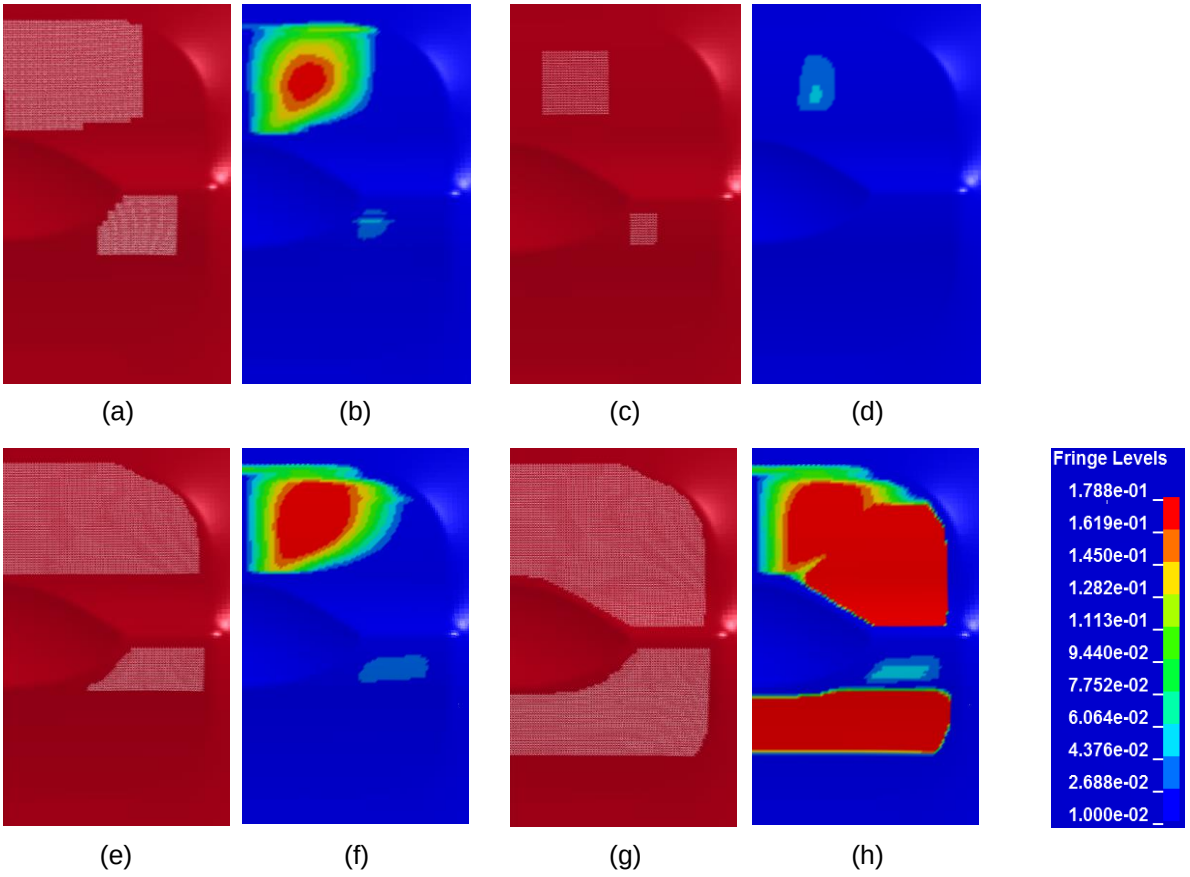

Fig.9: Influence of the set size for the stoning on the size and shape of detected surface deflections.

6.2 Experimental Validation

Figure 10 shows the formed part for the experimental validation. It is necessary to use the stoning method to make surface deflections visible.

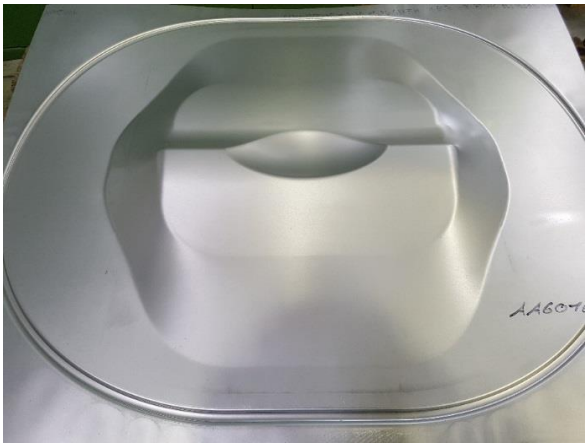

Fig.10: Formed part

To validate the deep drawing and springback simulation, the strain was evaluated on the physical part as well as on the numerical result. The results for the true major strain are shown in Figure 11 and the results of the true minor strain are shown in Figure 12. Both Figures show a good agreement between the experimental (a) and numerical (b) results.

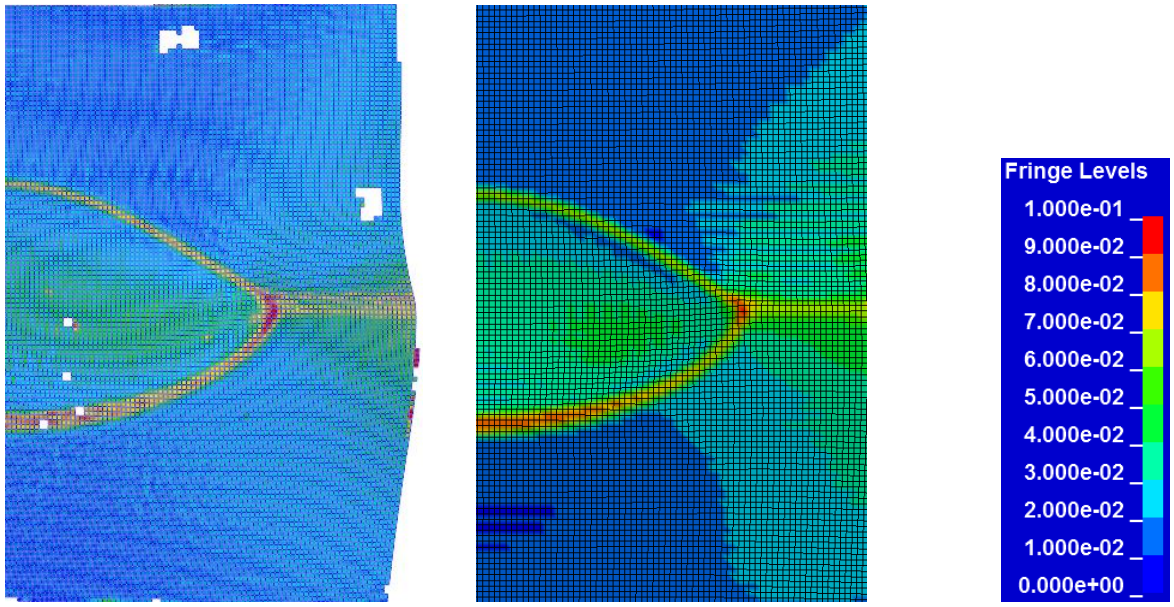

(a) (b)

Fig.11: Major strain distribution of the experimental results (a) and the numerical results (b)

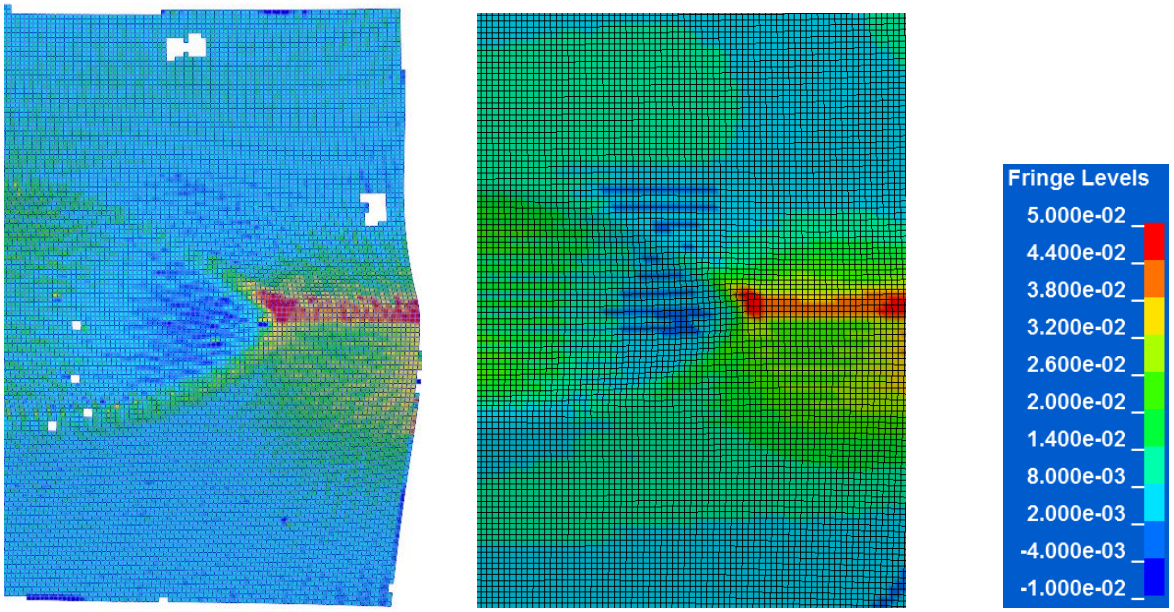

(a) (b)

Fig.12: Minor strain distribution of the experimental results (a) and the numerical results (b)

To validate the detection of surface deflections, a virtual stoning method was applied to the numerical results and a real stone of the same size was used for the physical parts. Both stones have a length of 100 mm and a width of 1 mm. The sets in Figure 9 (a) are used to detect the surface deflections on the numerical results. Figure 13 shows the results of the stoning. The surface deflections in area B and area A are shown in Figure 13 (a) and (b) correspondingly. Figure 13 (c) shows the numerical result. The white contours represent the results of the physical part. It can be observed that both surface deflections can be detected quite well. The detection of the surface deflection in area B can be improved by choosing the exact size of the set for the numerical investigation.

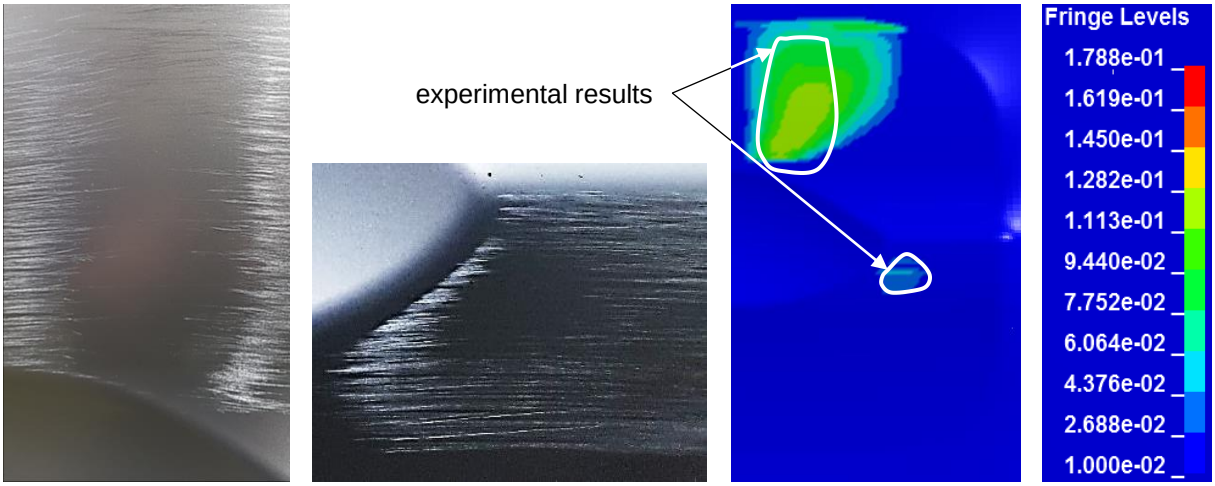

(a) (b) (c)

Fig.13: Detection of surface deflections with a stone with length of 100 mm and a width of 1 mm on a physical part in area B (a) and A (b) and in the numerical results (c)

7 Future Work

Since the results show that the length of the stone has a high impact on the detected surface deflection the next step includes the investigation of the influence of different stone lengths on the detected surface deflections on physical parts. In addition, a slightly modified part geometry without surface deflections will be evaluated experimentally and numerically to analyze if the stoning method is able to correctly detect no surface deflections for a part with none present.

8 Summary

This paper shows that it is possible to detect surface deflections with the keyword ***CONTROL_FORMING_STONING**. A simulation with the recommended settings leads to good results. However, the set for the application of the stoning must be chosen very carefully as it has a major influence of the detected shape of the surface deflections.

9 Acknowledgments

We extend our sincere thanks to the European Research Association for Sheet Metal Working and the German Federation of Industrial Research Associations for financing our investigations as part of the program for the furthering of the Industrial Collective Research by the Federal Ministry for Economic Affairs and Energy.

10 Literature

[1] Hazra, S.; Roy, R.; Williams, D.; Aylmore, R.; Hollingdale, D.: A novel inspection method for determining the cosmetic quality of automotive skin panels, Journal of Materials Processing Technology, 213, 2013, p. 2049-2063

[2] Fukumura, M.; Yamasaki, Y.; Inage, D.; Fujita, T.: Finite Element Simulation of Surface Defects in the Automobile Door Outer Panel, AIP Conference Proceedings, 712, 2004, p. 1917-1922

[3] Anderson, A.: Evaluation and Visualization of Surface Defects – a Numerical and Experimental Study on Sheet-Metal Parts, Numisheet, 2005, p. 113-118

[4] Port, A.; Thuillier, S.; Manach, P.: Occurrence and numerical prediction of surface defects during flanging of metallic sheets, International Journal of Material Forming, 2009, p. 215-223

[5] Weinschenk, A.; Volk, W.: Systematic investigation of geometrical parameters‘ influence on the appearance of surface deflections in sheet metal forming, Journal of Physics: Conference Series, 734, 2016, p. 032004

[6] LS-DYNA KEYWORD USER’S MANUAL VOLUME I, 2016